

# Performance of multi-wall carbon nanotubes modified by chitosan and EDTA in the removal of Direct Blue 15 dye from aqueous solutions

Mohammad Shakak Nalus<sup>1</sup>, Reza Rezaee<sup>2,✉</sup>, Mahdi Safari<sup>2</sup>, Esmail Ghahramani<sup>2</sup>, Behzad Shahmoradi<sup>2</sup>, Yahya Zandsalimi<sup>2</sup>

1. Student Research Committee, Kurdistan University of Medical Sciences, Sanandaj, Iran
2. Environmental Health Research Center, Research Institute for Health Development, Kurdistan University of Medical Sciences, Sanandaj, Iran

**Date of submission:** 23 March 2020, **Date of acceptance:** 23 May 2020

## ABSTRACT

Dyes are considered to be important pollutants in different industries (e.g., textile) and contain various organic materials with complicated structures. These compounds are mainly carcinogenic and toxic and less biodegradable when discharged into the environment. The present study aimed to investigate the performance of multi-wall carbon nanotubes (MWCNTs) modified by chitosan and EDTA in the removal of Direct Blue 15 dye from aqueous solutions. MWCNT was synthesized and characterized using the BET, zeta potential, DLS, SEM, and FTIR techniques. The effects of key parameters including pH, adsorbent dose, initial dye concentration, and contact time were also evaluated. The experimental data of the adsorption process were analyzed using the Langmuir and Freundlich models. With the increased contact time, the removal efficiency of the dye improved, while the increased pH, initial dye concentration, and adsorbent dose led to the reduced dye removal efficiency. With the optimum values of pH (7), contact time (60 min), adsorbent dose (0.5 g/L), and initial dye concentration (60 mg/L), the maximum adsorption capacity was determined to be 114.42 mg/g. According to the results, the adsorption process using the modified MWCNT followed the Langmuir model and pseudo-second-order kinetics.

**Keywords:** Parameter optimization, Adsorption, Modification, Chitosan, EDTA

## Introduction

Environmental pollution due to various sources has been a pressing issue in recent years. The textile industry is a basic industry and a major source of environmental pollution. Approximately 700,000 tons of dyes are synthesized worldwide each year, 50% of which include azo dyes.<sup>1</sup> Azo dyes contain one or more azo bonds (-N=N-) in their structure

and are considered to be the most significant which include azo which include azo synthetic dyes that are extensively produced and have numerous applications in various industries, especially the textile and dyeing industries.<sup>2</sup> Approximately 15% of the annual production of synthetic dyes enters textile effluents during the dyeing process. The discharge of dye-laden wastewater into the environment hinders light from penetrating the aquatic ecosystems, thereby slowing down the photosynthesis process.<sup>3</sup> Moreover, some azo dyes and their impurities (e.g., amines) are toxic and even carcinogenic to various organisms.<sup>4</sup>

✉ Reza Rezaee  
rezaee.eng@gmail.com

**Citain:** Shakak Nalus M, Rezaee R, Safari M, Ghahramani E, Shahmoradi B, Zandsalimi Y. Performance of multi-wall carbon nanotubes modified by chitosan and EDTA in the removal of Direct Blue 15 dye from aqueous solutions. J Adv Environ Health Res 2020; 8(2): 143-154

With the improvement of the textile dyeing industry, new dyes are injected into the market every day with better dyeing qualities. Due to the structural stability of these dyes, such improvement has caused these materials to resist biological and even chemical decomposition. Consequently, several researchers have attempted to find new methods to eliminate dyes from textile wastewater.<sup>5</sup>

The treatment of the wastewater containing dyes is regularly performed using physicochemical and biological techniques.<sup>6</sup> The conventional methods of textile wastewater treatment involve several steps, which are subjected to the product manufacturing process specifications. The treatments often comprise of coagulation and flocculation processes, which could be used individually or in combination with biological filtration processes to remove suspended solids and organic matters and advance dye removal from textile wastewater. One of the drawbacks of such treatments is the formation of high quantities of sludge that is brimmed with dyes and pollutants, which is considered highly challenging to meet environmental standards.<sup>4</sup> Furthermore, biological treatment,<sup>7</sup> ozonation,<sup>8</sup> chemical oxidation and photocatalytic processes,<sup>9</sup> membrane processes,<sup>10</sup> nanoparticles,<sup>11</sup> and photochemical and enzymatic treatment processes<sup>12</sup> have been employed to degrade dyes from textile effluents, and each process has specific advantages and disadvantages.<sup>13</sup>

Adsorption processes are among the practical methods of dye removal from textile wastewater.<sup>14</sup> These processes are highly efficient in the removal of dyes, odors, and organic matters from wastewater.<sup>15</sup> Additionally, the adsorption process is a reliable purification technique for the reduction of investment costs owing to its ease of design and operation and no sensitivity to toxic compounds.<sup>16</sup> Some of the adsorbents used in the treatment of dyed wastewater include activated carbon,<sup>17</sup> porous carbon,<sup>18</sup> clay,<sup>19</sup> biopolymers (e.g., chitosan),<sup>20</sup> and agricultural waste.<sup>21</sup> In this method, the dye

compounds in wastewater are readily transformed to the solid phase, and the adsorbent could be restored and reused.<sup>22</sup> Recently, carbon allotropies such as carbon nanotubes (CNTs) and graphene oxide have been broadly used for the removal of various pollutants (especially dyes) due to their high surface-to-volume proportion and high adsorption capacity.<sup>23</sup> CNTs are composed of one-atom-thick, hollow, cylindrical carbon plates, and their unique properties (e.g., high cross-sectional area, porous and layered structure) make CNTs an effective and practical adsorbent for the removal of various pollutants, especially organic pollutants.<sup>24</sup>

As a non-toxic, biodegradable, and environmentally friendly natural biopolymer, chitosan is considered to be a proper alternative to bleaching as a sorbent in the textile industry. Chitosan is extensively utilized as a biosorbent owing to its chelating behavior and cost-efficiency compared to commercial adsorbents.<sup>25</sup> In addition, chitosan could enhance the efficiency of the adsorption process by modifying or functionalizing the surface of carbon nanotubes through the improvement of interfacial interactions, including chemical, physical, and mechanical bonds.<sup>26</sup>

The present study aimed to investigate the efficiency of the multi-wall carbon nanotubes (MWCNTs) modified with EDTA and chitosan in the removal of Direct Blue 15 dye from aquatic solutions.

## Materials and Methods

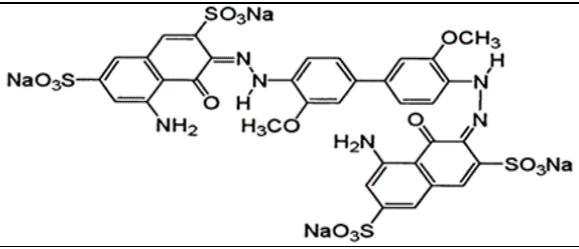
### *Materials and reagents*

This experimental-laboratory study was conducted to define the efficiency of the EDTA-chitosan-modified MWCNT composites in a batch mode in the removal of Direct Blue 15 dye from aquatic environments. The MWCNTs were purchased from the Research Institute of Petroleum Industry, Iran, and Direct Blue 15 was provided by Alvan Sabet Co. in Hamadan, Iran (Table 1). The maximum adsorption wavelength of the Direct Blue 15 dye was determined using a UV/Vis spectrophotometer (model: DR-5000-HACH).

To determine the location of the functional groups on the surface of the nanotubes and arrangement of their crystal lattice, the scanning electron microscopy (SEM; TSCAN Mira3 LMH) was used, and a Fourier transform infrared (FT-IR) spectroscope (model: Tensor 27, Bruker, Germany) was utilized for the characterization of the surface

properties and confirmation of the functional groups before and after the modification of the adsorbent within the range of 500-4,000  $\text{cm}^{-1}$ . In this research, X-ray diffraction XRD, dynamic light scattering (DLS), surface area (BET), and the zeta potential of the modified MWCNT nanocomposites were also determined.

Table 1. Properties of Direct Blue 15

Chemical structure	
Molecular formula	$\text{C}_{34}\text{H}_{24}\text{N}_6\text{Na}_4\text{O}_{16}\text{S}_4$
Type	Double azo class
Molecular weight	992.81 (g/mol)
$\lambda_{\text{max}}$	610 nm

### Adsorbent preparation

#### Modification of the MWCNTs with ethylene diamine tetraacetic acid (EDTA)

Initially, 5 g of EDTA-2Na was dissolved in 100 mL of distilled water. Afterwards, 100 mL of the suspension containing 1 g of the MWCNTs was slowly added at room temperature, and the solution was stirred on a high-speed magnetic stirrer for 3.5 h.

#### Synthesis of the MWCNT composites modified with chitosan and EDTA

To synthesize the nanocomposite, 2 g of chitosan was added to 100 mL of 3% acetic acid. Following that, the chitosan solution was mixed for 1 h at high speed, and the solution was gently added to the prepared mixture of EDTA-2Na and MWCNTs at room temperature. To ensure complete dissolution, the solution was placed in a 37-kHz ultrasonic device for 20 min, followed by stirring at room temperature for 16 h. Finally, the solids were separated by centrifugation, washed repeatedly with distilled water, and dried under vacuum at the temperature of 60  $^{\circ}\text{C}$ .<sup>27</sup>

### Adsorption experiments

Initially, the Direct Blue 15 dye powder

was placed in oven at the temperature of 110  $^{\circ}\text{C}$  for 2 h. Following that, the stock solution of the dye (1,000 mg/L) was prepared. Several parameters were assessed based on the pretests and results of similar studies, including pH, adsorbent dose, initial dye concentration, and contact time. The one-factor-at-a-time procedure was applied to optimize the parameters. To adjust the pH of the samples, 0.1-N NaOH and HCl were used. The removal efficiency of the system was recorded with the initial dye content of 10, 40, 60, 100, and 200 mg/L, pH of 3, 5, 7, 9, and 11, MWCNT dose of 0.25, 0.5, 1, 2, and 3 g/L and contact time of 10, 30, 45, 60, 90, and 120 min. In all the experiments, the stirrer speed was set at 200 rpm. After the centrifugation of the samples, the dye residue was measured using the UV/Vis spectrophotometer ( $\lambda_{\text{max}}$ : 610 nm).<sup>28</sup> The dye removal efficiency was calculated using Eq. 1, as follows:

$$R(\%) = \frac{(c_0 - c_e)}{c_0} \times 100 \quad (1)$$

The adsorption capacity of the modified carbon nanotubes for various dye concentrations was determined using Eq. 2, as follows:

$$q_e = \frac{(c_0 - c_e)}{W} \quad (2)$$

where,  $c_0$  and  $c_e$  are the initial and equilibrium concentrations (mg/L) of the dye after adsorption, respectively, and  $W$  shows the adsorbent mass in the solution volume (g/L).

## Results and Discussion

### Structure and morphology of the nanoparticles

Fig. 1 depicts the results of the FTIR of the modified MWCNTs. The FTIR spectroscopy of the virgin adsorbent (A), modified adsorbent (B), and virgin chitosan (C) has also been shown in the same figure, confirming the effective modification of the

carbon nanotubes. In diagram B, the absorption peak was estimated at  $13,440 \text{ cm}^{-1}$  due to the presence of stretch O-H groups. The peaks observed within the range of  $2,922\text{--}2,904 \text{ cm}^{-1}$  could be suggestive of stretch C-H vibrations, which were amplified after the adsorbent modification. In diagram C, the peak of  $1,637 \text{ cm}^{-1}$  was observed in the presence of stretch  $\text{-C}=\text{C}$ -groups, and the peak corresponding to  $1,442 \text{ cm}^{-1}$  could express the presence of bend C-H groups and stretch C-Os. In addition, the peak observed at  $1,053 \text{ cm}^{-1}$  was related to crude chitosan, and the peaks corresponding to  $880 \text{ cm}^{-1}$  indicated the presence of C-H groups on the surface of the carbon nanotubes after modification.<sup>29,30</sup>

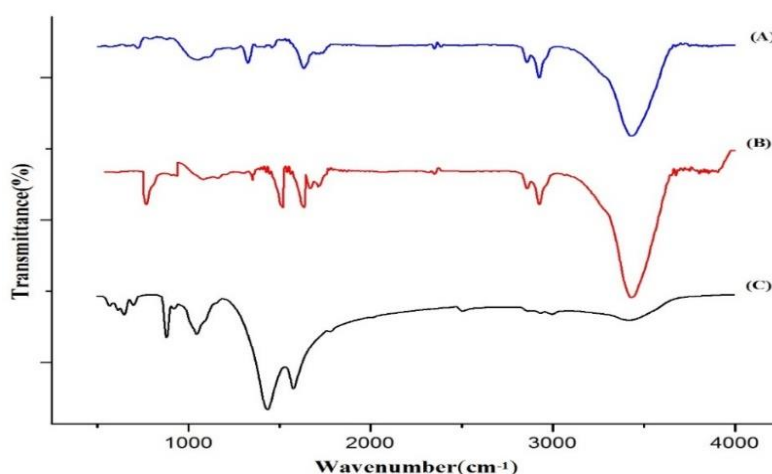


Fig. 1. FTIR spectroscopy of (A) virgin adsorbent, (B) modified adsorbent, and (C) virgin chitosan

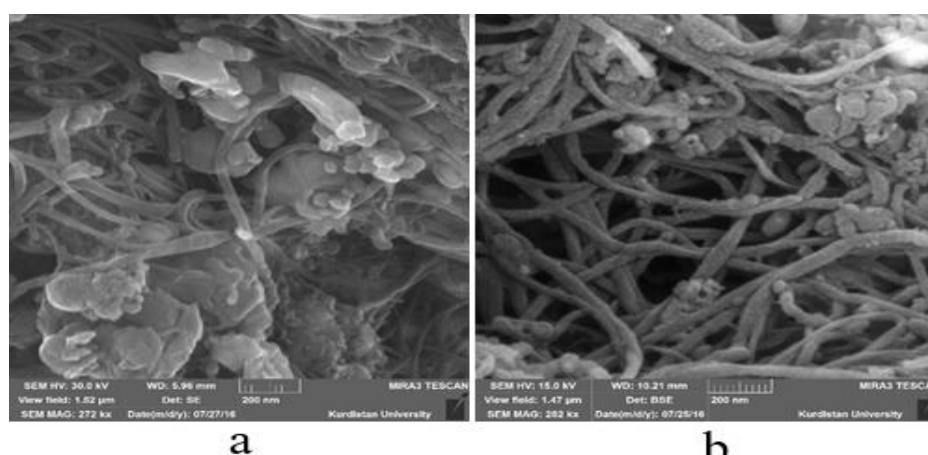


Fig. 2. SEM image of raw MWCNT (a) and chitosan-modified MWCNT (b)

Fig. 2 shows the SEM images of the CNs and chitosan-modified MWCNT nanocomposites. Accordingly, the CNs had

low porosity and tubular texture, while the composite surface was rough and porous. This characteristic of the composite surface is

essential to surface adsorbents as it shows the expansion of the surface area and high absorption efficiency. In addition, the roughness and high porosity of the composite causes the hydrophobicity of the adsorbent surface.

Fig. 3 shows the XRD image of the CNTs and chitosan-modified MWCNT nanocomposites at the degree of 10-90. The XRD images were employed to validate the crystalline structure and purity of the nanoparticles, measure the average distances between the layers and atomic series, and determine the location of the single crystal or grain. Although CNT is considered to be a non-crystalline material, its periodic structure leads to distinct X-ray scattering.<sup>31</sup> As depicted in the XRD scattering pattern, no significant peak was observed before the modification, with the exception of the CNT peak. Through the modification and addition of chitosan, the peaks within the range of 30-50  $cm^{-1}$  were

added. Figs. 4 and 5 depict the results of DLS and zeta potential for the CNTs and chitosan-modified MWCNT nanocomposites. The DLS revealed that the particle size in the raw CNTs was within the range of 120-300 nanometers, while it was approximately 160-500 nanometers in the prepared nanocomposites; as can be deduced, the addition of chitosan to the CNTs expanded the size.

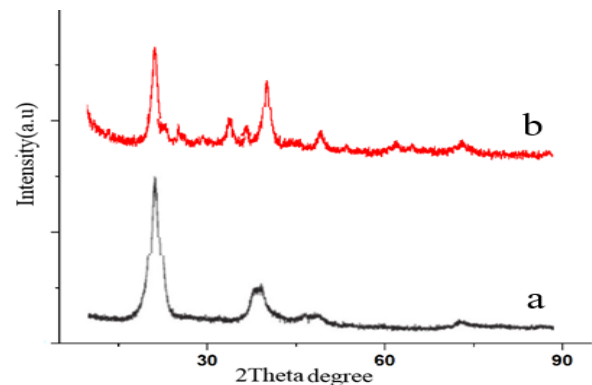


Fig. 3. XRD of (A) raw MWCNT and (B) chitosan-modified MWCNT nanocomposites

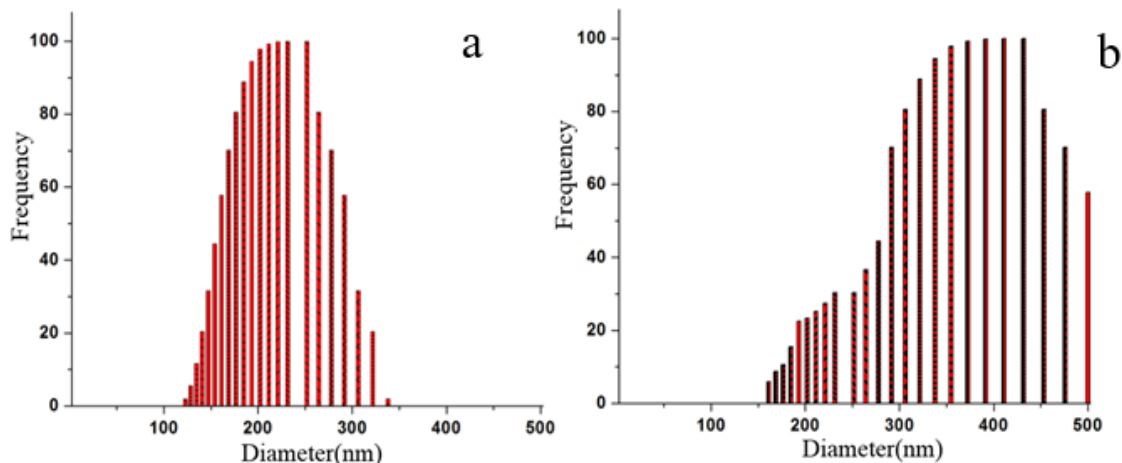


Fig. 4. DLS of (a) raw MWCNT and (b) chitosan-modified MWCNT nanocomposites

### Zeta potential

The zeta potential is essential to the investigation of the properties of colloidal suspensions. In the present study, the electrical zeta potential of the raw MWCNT and chitosan-modified MWCNT nanocomposite was measured at the optimum pH. For this purpose, a suspension of 0.01 g of the adsorbent in 5 mL of distilled water was prepared, and all the samples were irradiated with ultrasonic waves for 15 min before the

zeta potential measurement. The results of the zeta potential (Fig. 5) confirmed that the zeta potential and motion increased in the contaminated nanoparticles. Therefore, the zeta potential in the raw MWCNT and chitosan-modified MWCNT nanocomposites was calculated to be 0.43 and -0.23 mV, respectively. Evidently, adsorption modification enhanced both the surface area and surface charge.



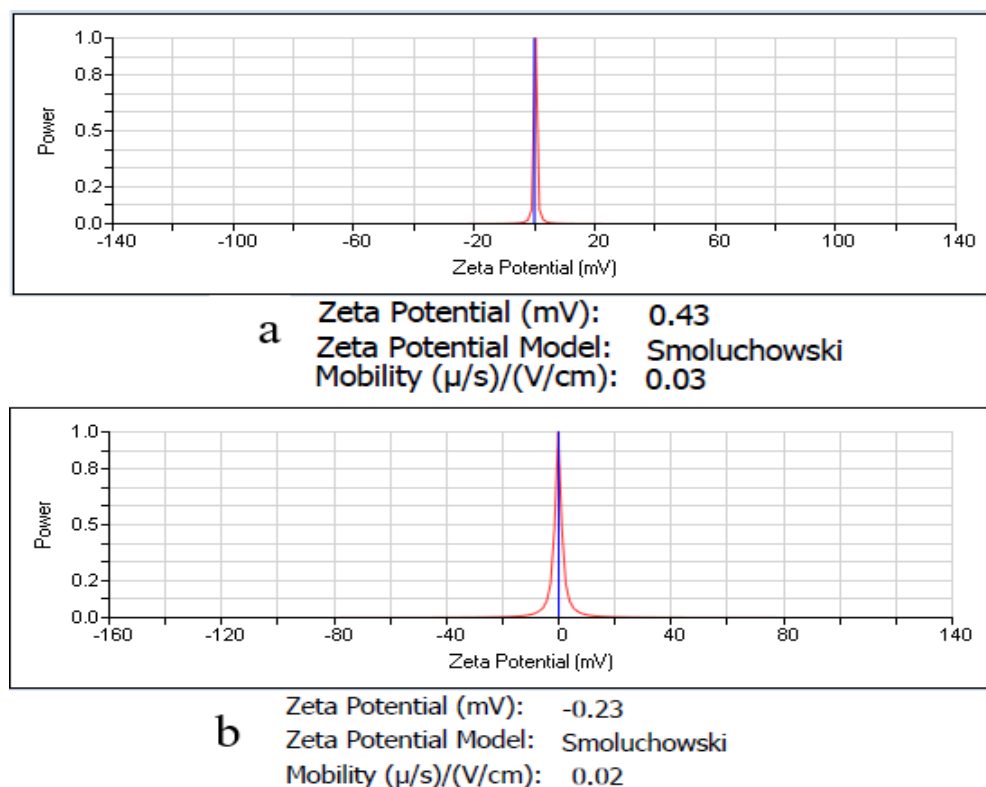


Fig. 5. Zeta potential of (A) raw MWCNT and (B) chitosan-modified MWCNT nanocomposites

### BET

Table 2 shows the results of the BET analysis for the raw MWCNT and chitosan-modified MWCNT nanocomposites. Accordingly, the composite holes and surface of the chitosan-modified MWCNT nanocomposite were more reliable compared to the raw MWCNTs, which in turn led to the reduction of the surface area. The findings of the current research in this regard are consistent with the previous studies.<sup>32</sup>

Table 2. BET of raw MWCNT and chitosan-modified MWCNT nanocomposites

Sample	SBET ( $\text{m}^2/\text{g}$ )
Raw MWCNT	161
Chitosan-modified MWCNT nanocomposite	139

### Effects of various parameters on the adsorption process

#### pH solution

As is known, pH is a critical parameter in the adsorption process for the removal of environmental pollutants. Fig. 6 depicts the evaluation of the impact of pH on the removal efficiency of the Direct Blue 15 dye using the

EDTA/chitosan-modified MWCNT adsorbent. With the increased pH, the removal efficiency decreased substantially, so that at pH=3, the dye removal efficiency was estimated at 99%, while it increased to 62% at pH=11. Therefore, it could be inferred that at acidic pH, the adsorbent had a higher efficiency in the removal of Direct Blue 15, while at the acidic pH=3, the adsorption efficiency was highest. The adsorption rate was observed to be high at neutral pH, and due to economic and environmental issues, pH=7 was selected as the optimum value.

In adsorption processes, the pH of the solution may play a key role in the adsorption capacity due to the impact of the solution chemistry, adsorbent surface charge, and functional groups. As is observed in Fig. 6, the maximum acid removal occurred at acidic pH. Dye adsorption at high pH is due to the presence of hydroxyl functional groups and its association with the pH of the reaction medium. As is shown in Fig. 1 (B) and considering the presence of hydroxyl functional groups in the nanocomposite structure, the increased pH increased the bond

between the OH groups on the adsorbent surfaces, resulting in the negative charge.<sup>33</sup> Since Direct Blue 15 is anionic with a negative charge in aqueous solutions and NaSO<sub>3</sub> group is also present in its structure, this dye is dissolved in water to the Na<sup>+</sup> cation and SO<sub>3</sub><sup>-</sup> anion, adsorbing the negative charge of the medium. Therefore, higher pH led to the increased negative charge adsorption locations and reduced positive charge sites, thereby decreasing the dye removal efficiency. Effective dye removal occurs when the positive surface charge environment is appropriate.<sup>34</sup> In a research conducted by Maleki *et al.* to eliminate reactive blue dye 19 using natural and modified zeolites, both sulfuric acid and phosphoric acid modified the sorbents, and the removal efficiency decreased with increased pH. This finding is consistent with the results of the present study.<sup>35</sup>

#### Adsorbent dosage

In order to determine the impact of the adsorbent dosage on the dye removal, some experiments were performed with the adsorbent dosage of 10-200 mg/L, pH of 7, contact time of 60 min, and initial dye content of 60 mg/L (Fig. 7). According to the obtained results, the increased adsorbent dose was associated with the higher efficiency, followed by a reduction. At the adsorbent dose of 0.5 g/L, the dye removal efficiency at the concentrations of 10 and 200 mg/L was

estimated at 96 and 87%, respectively. However, increasing the adsorbent dosage to 3 g/L caused the removal efficiency to decrease by 91 and 77%, respectively. Consequently, the adsorbent dosage of 0.5 g/L was considered optimal. By increasing the adsorbent dosage to a certain level, the removal efficiency increased for all the dyes. When the adsorbent further increased, the dye removal efficiency remained constant and eventually declined. By increasing the adsorbent dosage from 0.25 to 0.5 g/L for the dye at the concentration of 60 mg/L, the removal efficiency increased from 76.62 to 90%, which could be due to the increment in the adsorbent dosage as it made more surface area and more adsorption sites available to the dye molecules, thereby increasing the dye removal efficiency.

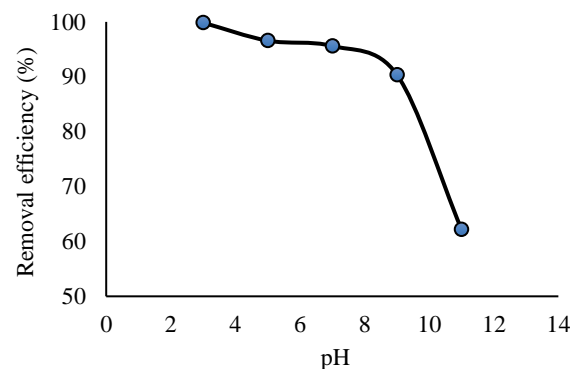


Fig. 6. Effect of solution pH on removal efficiency of Direct Blue 15 using EDTA/chitosan-modified MWCNT nanocomposite (adsorbent dose: 0.5 g/L, contact time: 60 min, initial dye concentration: 60 mg/L)

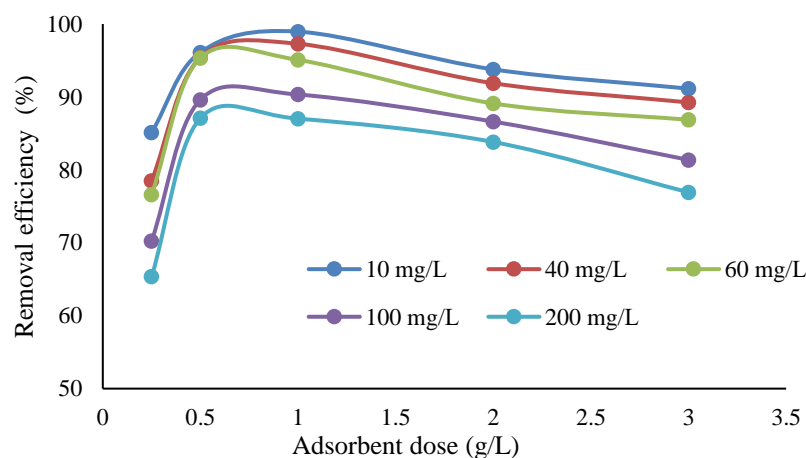


Fig. 7. Effect of adsorbent dose on removal efficiency using EDTA and chitosan-modified MWCNT (pH: 7, contact time: 60 min, dye content: 60 mg/L)

### Initial dye concentration

Fig. 8 shows the impact of the initial Direct Blue 15 concentration on the removal efficiency by the EDTA/chitosan-modified MWCNTs adsorbent. Fig. 2 depicts the correlation of dye adsorption ( $q_e$ ) with the increased concentration of the Direct Blue 15 dye. According to the findings, the dye removal efficiency declined with the increased initial dye concentration. However, the actual amount of the dye absorbed per unit mass of the nanotubes ( $q_e$ ) increased at higher initial dye concentrations. As can be seen in Fig. 5, at the initial dye concentration of 10 mg/L, the removal efficiency was approximately 96%, while at the concentration of 200 mg/L, the removal efficiency declined to approximately 87%. Furthermore, the removal efficiency decreased at higher initial dye concentrations. At the initial dye concentration of 10 mg/L, the removal efficiency was estimated at 96%, while at the concentration of 200 mg/L, the removal efficiency declined to approximately 87%. This reduction in the removal efficiency

could be due to the saturation of the vacant active sites on the adsorbent surface at higher dye concentrations.<sup>38</sup>

At high dye concentrations, the quantity of the adsorbed dye on the carbon nanotubes increased (Diagram 2), so that the dye absorption capacity at the concentration of 10 mg/L was 19.22 mg/g, and at the concentration of 200 mg/L, it reached 348.32 mg/g; this could be attributed to the increment in the concentration gradient force.<sup>39</sup> In a study by Rahmani *et al.* regarding the removal of the Reactive Black 5 dye using adsorption on anionic ion exchange resin, the removal efficiency decreased from 99 to 24% when the initial dye concentration increased from 50 to 300 mg/L.<sup>40</sup> This finding is consistent with the results of the present study. In another research by Luo *et al.* regarding the adsorption of natural red dye on halloysite nanotubes, the adsorption capacity increased from 24.92 to 65.69 mg/g with the increased dye concentration from 50 to 400 mg/L at 318 K. This is in line with the current research.<sup>41</sup>

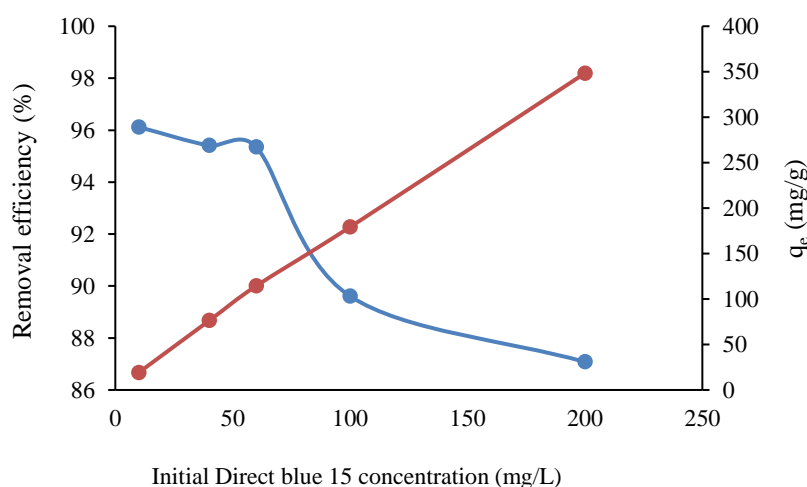


Fig. 8. Effect of initial dye concentration on removal efficiency using EDTA and chitosan-modified MWCNT (pH: 7, contact time: 60 min, dye content: 60 mg/L)

### Contact time

Fig. 9 depicts the rate of dye absorption at different contact times. The obtained results confirmed that with the increased contact time, the dye removal efficiency initially increased, reaching balance within nearly 1 h. During 10 min of contact, the dye absorption was

estimated at 104 mg/g, while with the increased contact time to 60 min, the absorption rate reached 114 mg/g. Following that, the slope of the graph decreased, so that with the increased contact time to 120 min, the dye absorption reached approximately 115 mg/g.



To assess the effect of contact time, the initial dye concentration of 60 mg/L, optimum pH (7), and the obtained adsorbent dosage were considered. According to the findings, the dye adsorption capacity increased with the increased contact time, confirming that dye adsorption occurred within less than 1 h at high speed, so that the dye absorption rate of approximately 104 mg/g was observed at 10 min of exposure. This high amount was due to the fact that more unsaturated adsorption sites became available to the dye molecules during this contact duration, so that the dye adsorption rate of approximately 104 mg/g was observed at 10 min of exposure. After the contact time of 1 h, the slope of the graph decreased, so that with the increased contact time to 120 min, the dye adsorption reached approximately 115 mg/g.

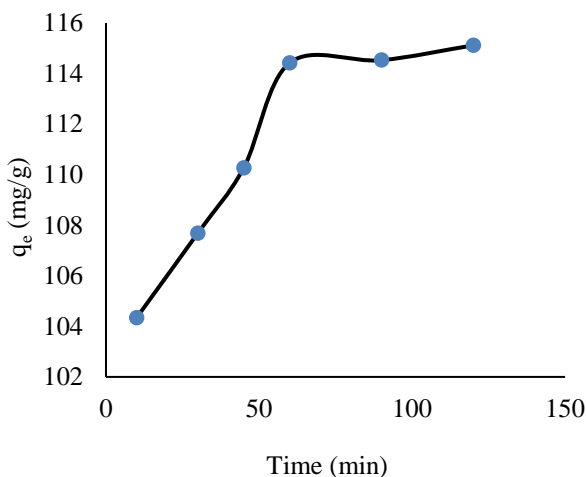


Fig. 9. Effect of contact time on removal efficiency using EDTA and chitosan-modified MWCNT (pH=7, adsorbent dose: 0.5 g/L, dye content 60 mg/L)

The reduction of the adsorption rate with the increased contact time was due to the saturation of the active sites on the adsorbent surface and increased repulsive force. As a result, the equilibrium time for the adsorption of the Direct Blue 15 dye onto the MCNs was 1 h in the present study. The findings reported by Shirmardi *et al.* are in line with the results of the present study.<sup>42</sup> Furthermore, the study by Malakootian *et al.* indicated that within the first 60 min, the uptake of anionic surfactant by modified Leica increased and reached balance

within 90 min. However, the absorption rate did not vary significantly for more than 90 min,<sup>43</sup> which is consistent with the results of the present study.

### Adsorption isotherms

Adsorption isotherms provide vital data to optimize the absorption system configuration. In the current research, the Langmuir and Freundlich models, which are among the most commonly employed adsorption isotherm models, were used to characterize the adsorption of the Direct Blue 15 dye onto the EDTA and chitosan-modified MWCNT.

The Langmuir isotherm is based on the premise of monolayer adsorption on a homogeneous structure adsorbent, assuming that all the sites have the same adsorption energy and are equal.<sup>44</sup> The linear form of the Langmuir equation is as Eq. 3:

$$\frac{C_e}{q_e} = \frac{1}{q_m k_L} + \frac{1}{q_m} C_e \quad (3)$$

where  $q_e$  is the amount of the adsorbed dye for a given amount of the consumed adsorbent (mg/g),  $C_e$  shows the equilibrium concentration of the solution (mg/L),  $q_m$  is the maximum amount of the dye required to form a singular layer (mg/g), and  $k_L$  represents the Langmuir equilibrium absorbance constant (l/mg).

The Freundlich isotherm is an experimental equation associated with heterogeneous adsorbent surfaces, the linear form of which is expressed, as Eq. 4:

$$\ln(q_e) = \ln(K_f) + \frac{1}{n} \ln(C_e) \quad (4)$$

where the Freundlich  $k_f$  and  $n$  adsorption constants show the absorption capacity and intensity, respectively. In the current research, the results of the isotherm studies (Fig. 10, Table 3) revealed that the adsorption of the Direct Blue 15 dye on the EDTA and chitosan-modified MWCNT complied more with the Freundlich isotherm model, and its correlation-coefficient ( $R^2$ ) was higher than the Langmuir model. This finding indicated that the adsorption process was performed in the uncertain and heterogeneous locations of the adsorbent sites.

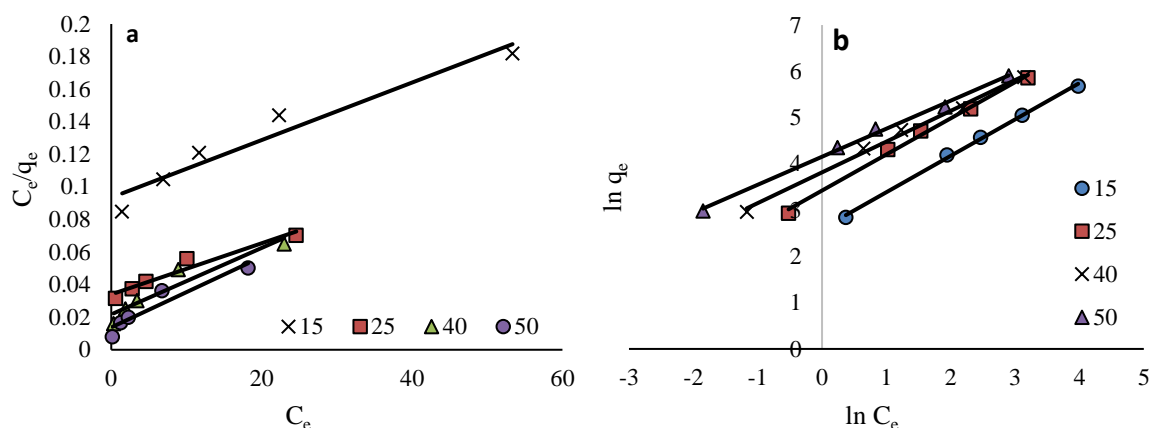


Fig. 10. Adsorption isotherms: (a) Langmuir model, (b) Freundlich model

Table 3. Variables of adsorption isotherms of Direct Blue 15 on EDTA and chitosan-modified MWCNT

T (°C)	Isotherm model						
	Frundlich			Langmuir			
	n	$K_f$	$R^2$	$q_m$	$R_L$	$K_L$	$R^2$
15	1.27	13.46	0.9975	555.55	0.46	0.019	0.9420
25	1.28	30.70	0.9945	625.00	0.26	0.047	0.9414
40	1.50	45.57	0.9940	500.00	0.15	0.092	0.9106
50	1.65	63.53	0.9957	454.54	0.09	0.160	0.9039

### Adsorption kinetics

In the current research, the equilibrium data were used to examine the reaction kinetics and their conformity with the pseudo-first- and pseudo-second-order kinetic equations. Eqs. 5 and 6 denote the first and second pseudo-linear Eqs., as follows:

$$\ln(q_e - q_t) = \ln(q_e) - k_1 t \quad (5)$$

$$\frac{t}{q_t} = \frac{1}{k_2 q_e^2} + \frac{1}{q_e} t \quad (6)$$

In Eqs. 5 and 6,  $k_1$  and  $k_2$  are the coefficients of velocity ( $\text{min}^{-1}$ ) and quadratic reaction constant ( $\text{g/mg min}$ ), respectively, and  $q_e$  and  $q_t$  show the adsorption capacity at the equilibrium and adsorption capacity at time  $t$ , respectively ( $\text{mg/g}$ ). The results and calculations of the kinetic equations in Table 3 and Figs. 9 and 10 indicate that the pseudo-second-order kinetic model was more accurate in describing the adsorption behavior of the dye molecules on the EDTA and chitosan-modified MWCNT. In a study by Nevine regarding the removal of the Direct Blue 106 dye using the activated carbon adsorbent made of pomegranate peel, the dye adsorption was reported to follow the pseudo-second-order kinetic model ( $R^2 \geq 0.99$ ).<sup>45</sup>

### Conclusion

According to the results, the modification of the MWCNT by chitosan and EDTA was significantly more effective in dye adsorption compared to the MWCNT. Therefore, MWCNT could be applied as a promising adsorbent for the removal of dyes from effluents.

### Acknowledgments

Hereby, we extend our gratitude to the Vice Chancellor of Research and Technology at Kurdistan University of Medical Sciences for the financial support of this research project (grant No. 1395/248).

### References

1. Luo X, Zhan Y, Huang Y, Yang L, Tu X, Luo S. Removal of water-soluble acid dyes from water environment using a novel magnetic molecularly imprinted polymer. *J Hazard Mater* 2011; 187(1-3): 274-82.
2. McKay G, Hadi M, Samadi MT, Rahmani AR, Solaimany Aminabad M, Nazemi F. Adsorption of reactive dye from aqueous solutions by compost. *Desalin Water Treat* 2011; 28(1-3): 164-73.
3. Bulut Y, Aydın H. A kinetics and

- thermodynamics study of methylene blue adsorption on wheat shells. *Desalination* 2006; 194(1-3): 259-67.
- Ghodsian M, Ayati B, Ganjidoust H. Determination of optimum amounts of effective parameters in reactive dyes removal using photocatalytic reactions by immobilized TiO<sub>2</sub> nano particles on concrete surface. *J Water Wastewater* 2013; 24(3): 45-53. [In Persian]
  - Lima EC, Royer B, Vagheti JC, Simon NM, Da Cunha BM, Pavan FA, *et al.* Application of Brazilian pine-fruit shell as a biosorbent to removal of reactive red 194 textile dye from aqueous solution: Kinetics and equilibrium study. *J Hazard Mater* 2008; 155(3): 536-50.
  - Vijayaraghavan K, Yun Y-S. Biosorption of C.I. Reactive Black 5 from aqueous solution using acid-treated biomass of brown seaweed *Laminaria* sp. *Dyes Pigm* 2008; 76(3): 726-32.
  - Punzi M, Anbalagan A, Börner RA, Svensson B-M, Jonstrup M, Mattiasson B. Degradation of a textile azo dye using biological treatment followed by photo-Fenton oxidation: Evaluation of toxicity and microbial community structure. *Chem Eng J* 2015; 270: 290-9.
  - Paździor K, Wrębiak J, Klepacz-Smółka A, Gmurek M, Bilińska L, Kos L, *et al.* Influence of ozonation and biodegradation on toxicity of industrial textile wastewater. *J Environ Manage* 2017; 195: 166-73.
  - Türgay O, Ersöz G, Atalay S, Forss J, Welander U. The treatment of azo dyes found in textile industry wastewater by anaerobic biological method and chemical oxidation. *Sep Purif Technol* 2011; 79(1): 26-33.
  - Liu M, Chen Q, Lu K, Huang W, Lü Z, Zhou C, *et al.* High efficient removal of dyes from aqueous solution through nanofiltration using diethanolamine-modified polyamide thin-film composite membrane. *Sep Purif Technol* 2017; 173: 135-43.
  - Mahvi AH, Ghanbarian M, Nasser S, Khairi A. Mineralization and discoloration of textile wastewater by TiO<sub>2</sub> nanoparticles. *Desalination* 2009; 239(1-3): 309-16.
  - Dehghani MH, Mesdaghinia AR, Nasser S, Mahvi AH, Azam K. Application of SCR technology for degradation of reactive yellow dye in aqueous solution. *Water Qual Res J Can* 2008; 43(2-3): 183-7.
  - Kabra K, Chaudhary R, Sawhney RL. Treatment of hazardous organic and inorganic compounds through aqueous-phase photocatalysis: A review. *Ind Eng Chem Res* 2004; 43(24): 7683-96.
  - Tsai WT, Chang CY, Wang SY, Chang CF, Chien SF, Sun HF. Cleaner production of carbon adsorbents by utilizing agricultural waste corn cob. *Resour Conserv Recycl* 2001; 32(1): 43-53.
  - Tseng R-L, Wu F-C, Juang R-S. Liquid-phase adsorption of dyes and phenols using pinewood-based activated carbons. *Carbon* 2003; 41(3): 487-95.
  - Yagub MT, Sen TK, Afroze S, Ang HM. Dye and its removal from aqueous solution by adsorption: A review. *Adv Colloid Interface Sci* 2014; 209: 172-84.
  - Malik PK. Dye removal from wastewater using activated carbon developed from sawdust: Adsorption equilibrium and kinetics. *J Hazard Mater* 2004; 113(1-3): 81-8.
  - Asouhidou DD, Triantafyllidis KS, Lazaridis NK, Matis KA, Kim S-S, Pinnavaia TJ. Sorption of reactive dyes from aqueous solutions by ordered hexagonal and disordered mesoporous carbons. *Micropor Mesopor Mat* 2009; 117(1-2): 257-67.
  - Jourvand M, Shams Khorramabadi G, Omidi Khaniabadi Y, Godini H, Nourmoradi H. Removal of methylene blue from aqueous solutions using modified clay. *J Bas Res Med Sci* 2015; 2(1): 32-41.
  - Chiou M-S, Li H-Y. Equilibrium and kinetic modeling of adsorption of reactive dye on cross-linked chitosan beads. *J Hazard Mater* 2002; 93(2): 233-48.
  - Wang XS, Zhou Y, Jiang Y, Sun C. The removal of basic dyes from aqueous solutions using agricultural by-products. *J Hazard Mater* 2008; 157(2-3): 374-85.
  - Bao Y, Zhang G. Study of adsorption characteristics of methylene blue onto activated carbon made by *Salix psammophila*. *Energy Procedia* 2012; 16: 1141-6.
  - Madrakian T, Afkhami A, Ahmadi M, Bagheri H. Removal of some cationic dyes from aqueous solutions using magnetic-modified multi-walled carbon nanotubes. *J Hazard Mater* 2011; 196: 109-14.
  - Lin D, Xing B. Adsorption of phenolic compounds by carbon nanotubes: Role of aromaticity and substitution of hydroxyl groups. *Environ Sci Technol* 2008; 42(19):

- 7254-9.
25. Crini G, Badot P-M. Application of chitosan, a natural aminopolysaccharide, for dye removal from aqueous solutions by adsorption processes using batch studies: A review of recent literature. *Prog Polym Sci* 2008; 33(4): 399-447.
  26. Moniruzzaman M, Winey KI. Polymer nanocomposites containing carbon nanotubes. *Macromolecules* 2006; 39(16): 5194-205.
  27. Zhang L, Luo H, Liu P, Fang W, Geng J. A novel modified graphene oxide/chitosan composite used as an adsorbent for Cr (VI) in aqueous solutions. *Int J Biol Macromol* 2016; 87: 586-96.
  28. Saroj S, Kumar K, Pareek N, Prasad R, Singh R. Biodegradation of azo dyes Acid Red 183, Direct Blue 15 and Direct Red 75 by the isolate *Penicillium oxalicum* SAR-3. *Chemosphere* 2014; 107: 240-8.
  29. Asfaram A, Fathi MR. Removal of direct red 12B dye from aqueous solutions by wheat straw: Isotherms, kinetics and thermodynamic studies. *J Color Sci Technol* 2013; 7(3): 223-35. [In Persian]
  30. Zare MA, Emadi M, Iranpoor M, Bazargan Lari R. Batch adsorption and removal of Methylene Blue (MB) from wastewater using Tassel as a cheap bioadsorbent. *J New Mater* 2014; 4(16): 81-98. [In Persian]
  31. Das R, Bee Abd Hamid S, Equb Ali M, Ramakrishna S, Yongzhi W. Carbon nanotubes characterization by X-ray powder diffraction—A review. *Curr Nanosci* 2015; 11(1): 23-35.
  32. Saudagar P, Dubey VK. Carbon nanotube based betulin formulation shows better efficacy against Leishmania parasite. *Parasitol Int* 2014; 63(6): 772-6.
  33. Li Y, Du Q, Liu T, Peng X, Wang J, Sun J, *et al.* Comparative study of methylene blue dye adsorption onto activated carbon, graphene oxide, and carbon nanotubes. *Chem Eng Res Des* 2013; 91(2): 361-8.
  34. Yao Y, Bing H, Feifei X, Xiaofeng C. Equilibrium and kinetic studies of methyl orange adsorption on multiwalled carbon nanotubes. *Chem Eng J* 2011; 170(1): 82-9.
  35. Maleki A, Mahvi AH, Rezaee R, Davari B. Removal of reactive blue 19 using natural and modified zeolites. *Iranian J Health Environ* 2013; 5(4): 519-30. [In Persian]
  36. Bazrafshan E, Kord Mostafapour F, Hosseini AR, Raksh Khorshid A, Mahvi AH. Decolorisation of reactive red 120 dye by using single-walled carbon nanotubes in aqueous solutions. *J Chem* 2012; 2013.
  37. Ghaneian MT, Momtaz M, Dehviri M. An investigation of the efficacy of Cuttlefish bone powder in the removal of Reactive Blue 19 dye from aqueous solutions: Equilibrium and isotherm studies. *J Community Health Res* 2012; 1(2): 68-78.
  38. Elwakeel KZ. Removal of Reactive Black 5 from aqueous solutions using magnetic chitosan resins. *J Hazard Mater* 2009; 167(1-3): 383-92.
  39. Duan J, Liu R, Chen T, Zhang B, Liu J. Halloysite nanotube-Fe<sub>3</sub>O<sub>4</sub> composite for removal of methyl violet from aqueous solutions. *Desalination* 2012; 293: 46-52.
  40. Rahmani AR, Asgari G, Farrokhi M, Shirzad siboni M. Removal of reactive black 5 (RB5) dye from aqueous solution using adsorption onto strongly basic anion exchange resin: Equilibrium and kinetic study. *Iran J Health & Environ* 2013; 5(4): 509-18. [In Persian]
  41. Luo P, Zhao Y, Zhang B, Liu J, Yang Y, Liu J. Study on the adsorption of neutral red from aqueous solution onto halloysite nanotubes. *Water Res* 2010; 44(5): 1489-97.
  42. Shirmardi M, Mesdaghinia A, Mahvi AH, Nasserri S, Nabizadeh R. Kinetics and equilibrium studies on adsorption of acid red 18 (Azo-Dye) using multiwall carbon nanotubes (MWCNTs) from aqueous solution. *E-J Chem* 2012, 9(4): 2371-83.
  43. Malakootian M, Yaghmaeian K, Momenzadeh R. Performance Evaluation of inorganic adsorbent Leca-modified of HCl for the removal of anionic surfactant from wastewater. *Sci J Ilam Univ Medic Sci* 2015; 23(4): 168-80. [In Persian]
  44. Kuo C-Y, Wu C-H, Wu J-Y. Adsorption of direct dyes from aqueous solutions by carbon nanotubes: Determination of equilibrium, kinetics and thermodynamics parameters. *J Colloid Interface Sci* 2008; 327(2): 308-15.
  45. Amin NK. Removal of direct blue-106 dye from aqueous solution using new activated carbons developed from pomegranate peel: Adsorption equilibrium and kinetics. *J Hazard Mater* 2009; 165(1-3): 52-62.